Coupling between proton binding and redox potential in electrochemically active macromolecules. The example of Polyaniline

Waldemar A. Marmisollé[1], *M. Inés Florit*[1] *and Dionisio Posadas*[1*]

Instituto de Investigaciones Fisicoquímicas Teóricas y Aplicadas (INIFTA). Facultad de Ciencias Exactas, Universidad Nacional de La Plata, CCT La Plata-CONICET. Sucursal 4, Casilla de Correo 16, 1900. La Plata, Argentina.

ABSTRACT. In this work it is investigated the coupling between the redox potential and the extent of proton binding in electrochemically active polymers, for the particular case of Polyaniline (Pani). To this purpose, the degree of oxidation of the polymer was measured by spectrophotometry changing the external potential applied to Pani films, in solutions of different *pH* values, as a function of the external applied potential. The knowledge of the oxidation degree for the different applied potentials allows determining the apparent formal redox potential. For Pani, in the absence of interactions between the redox centers, the apparent formal redox potential should be independent of the oxidation degree and it

---

[1] ISE member

[*] Corresponding author.

E-mail address: dposadas@inifta.unlp.edu.ar

should decrease linearly with the *pH* with a slope of 0.059 V, at room temperature. The values of the apparent formal redox potential, experimentally obtained, show that the *pH* dependence is not as expected from the redox equation. This fact implies interactions between the redox centers and some sort of coupling between the redox potential and the state of binding of the polymer. It is possible to estimate the interaction energy between the redox centers and also the acid dissociation constants of both, the oxidized and reduced forms, by employing a statistical mechanic model. The values obtained for both dissociation constants agree with some ones reported in the literature. The application of the model also allows explaining the observed relationship between the apparent formal redox potential and the electrolyte *pH*.

Keywords: Coupling. Proton Binding. Redox Potential Distribution. Polyaniline. Conducting Polymers

1. Introduction

Electrochemically active macromolecules (EAM) are substances that can be oxidized and reduced in a reversible way. These macromolecules, both natural and synthetic, have received a great deal of attention. The interest in natural EAM, mostly the metalloproteins, is due to its obvious importance in biochemical reactions [1]. On the other hand, the interest in synthetic EAM, mostly in polymers, is due to its potential applications in several fields [2–5].

These macromolecules can be characterized by several properties such as their redox potential, the binding state, the tension state and the extension of their screening. The redox potential is related to the possibility of the macromolecule to transfer electrons to a suitable redox couple in the same solution or to an electrode submitted to a suitable potential. The state of binding refers to the amount of bound species (mainly ions) on different sites of the macromolecule. The screening refers to the weakening of the electrostatics interactions between the fixed charged sites of the macromolecule due to the ionic atmosphere surrounding them. Finally, the state of tension here refers to the source of deformation that appears in the macromolecule even when it is isolated in the medium. Changes in the redox potential, net

charge of segments or ionic atmosphere can lead to small changes in distances or angles between adjacent parts (visualized as a simple covalent bond or a short segment of the chain that bevahes as a unity from a mechanical point of view) of the EAM. This deformation can be considered as driven by a tension, although the exact origin of the force implied may become elusive.

In a previous work [6], it was shown that a variety of experimental results in EAM can be explained by the existence of couplings among the state of tension, the state of binding, the extension of screening and the redox potential. That is, if one of these states changes, all the others will change too.

The vast majority of these macromolecules are polyelectrolytes. There are plenty examples of couplings of this type that can be attributed to its electrolytic nature. It is well known that polyelectrolytic macromolecules show couplings among the degree of binding, generally of protons, and its state of deformation [7–9] and screening [10–12]. Deformation can be also induced by redox potential changes [13,14], and changes in the ionic strength (screening) can modify the redox potential in both natural [15] and synthetic macromolecular systems [16]. Finally, a wide-spread coupling is that between the redox potential and the ion (mainly proton) binding [17–19]. This coupling is of paramount importance to understand the redox behaviour of proteins, substances in which their redox activity may depend on small changes of the binding ion activity [19–22].

Polyaniline (Pani) is a relatively simple synthetic polymer, as compared with natural electroactive macromolecules, for which the electrochemical behaviour is relatively well understood. The aim of this work is to theoretically interpret the experimental effect of proton binding on the redox potential of Pani by employing a modified statistical mechanics model.

Although simpler than many natural EAM, Pani presents an additional difficulty for the model: its redox potential depends directly on the proton activity in the solution, because protons participate in the redox reaction (Scheme 1). And, as protons also participate in a binding equilibrium with the macromolecule, the redox potential should indirectly depend on the solution *pH* through the coupling effects mentioned above.

In the present work, the coupling between proton binding and the redox potential of Pani, as a particular case of EAM, is experimental and theoretically studied. The experimental investigation of this coupling requires the determination of the oxidation degree of the polymer film in several conditions. Contrary to many systems, for conducting polymers as Pani, the oxidation degree can not be simply obtained from the voltammetric or chronoamperometric results beacuase the presence of a non-negligible pseudocapacitance distorts the electrochemical response [23,24]. So, in this work, the oxidation degree is obtained by UV- visible spectroelectrochemical measurements. On the other hand, a simple statistical mechanic model is developed to link the redox potential with the oxidation degree and the solution *pH*. The model allows the analysis of the experimental results to determine the proton binding constants of the reduced and the oxidized forms of the polymer, and also other parameters, such as differences of the interaction energy between the redox centres, as a function of the electrolyte *pH*.

2. Materials and Methods

Pani films were electro synthesized onto Indium Tin Oxide (ITO) plates (R_s = 5-15 Ω cm, Delta Technologies)**.** These plates were glued to a metallic contact with epoxy silver resin. The top and sides of the metallic plate were covered with an insulating varnish as shown in Fig. 1. The active area of the polymer film onto the ITO plate was around 1.0 cm^2. The electro synthesis was carried out by cycling the potential at 0.1 V s^{-1} between -0.200 V vs. a saturated calomel electrode (SCE) and a positive potential limit set at the beginning of the monomer oxidation (around 0.700 - 0.800 V). To improve the adherence and homogeneity of the film after a few cycles the positive potential limit was decreased. After the synthesis the film was washed with pure water and cycled in 3.7 M H_2SO_4 solution during some minutes and then introduced in the spectrophotometric cell. This was a square quartz cell (Spectrocell, 1 cm side) in which the electrode was inserted perpendicular to the light path. Inside the cell it was placed a Pt plate that serves as the counter electrode, and a fine capillary connected to an external reference electrode. This was also a SCE, which was employed throughout the work; all potentials in the text are referred to

it (see Fig. 1). The absorbance of the film electrodes was monitored over a period of several hours and no change was noticed, meaning the Pani film covering ITO plates was stable during that time.

Solutions were made of Milli-Q purified water and NaOH and H_2SO_4 (Carlo Erba, RPE-ACS). The latter were employed as received. A potentiostat TEQ-03 was employed for all the electrochemical experiments.

(Figure 1.)

Spectra were taken with an Agilent model 8453E diode array spectrophotometer in the spectral range comprised between 300 nm and 900 nm and in the potential range between -0.200 and 0.450 V.

Electrolytic solutions of different *pH* and constant ionic strength of 3.7·M of H_2SO_4 + $NaHSO_4$, were employed. The *pH* of these solutions was previously measured with a glass electrode adequate for acid media (Ross, Orion Research) by using a *pH*-meter (Cole-Palmer 59003-15).

Before starting the experiments with each one of the solutions of different *pH* values, the Pani- covered electrodes were polarized at -0.200 V during 20 minutes to completely reduce and age the Pani films [25,26]. Afterwards, the potential was increased in steps of 0.010 - 0.025 V and held at the corresponding potential value for 5 minutes, to reach the ionic equilibrium with the electrolytic solution. Then the spectrum was taken.

As a measure of the film thickness, it was employed the integrated charge from E = - 0.200 V up to 0.450 V, Q_T (0.45) [24]. Experiments were done with films of charge about Q_T (0.450) = 32 mC cm^{-2}.

3. Results

In Fig. 2 it is shown the voltammetric response of a typical Pani film between the potential limits -0.200 V and 0.450 V. During the potential scan the reduced form of Pani (Leucoemeraldine, L) is oxidized to the half oxidized form (Emeraldine, E).

The spectra of Pani for different applied potentials are shown in Fig. 3**.** These spectra show, three main characteristic bands in the wavelength range 300 - 900 nm. The band at 320 nm is attributed to the

$\pi \longrightarrow \pi^*$ transitions characteristic of the benzene ring units in the polymer. Also, it might be attributed to the band gap in the reduced polymer. This band is the main one for the L form; besides a second broad and small band is observed at about 850nm. As the polymer is oxidized, a band starts growing at about 400 nm, and the band with a maximum at around 850 nm in the reduced state, shows a gradual shift to 750 nm. These ones are attributed to the polarons and bipolarons associated to the formation of the quinonic units due to the oxidation of the amine to imine groups. Further discussions about the band assignations in Pani spectra are available in several works [27–30].

(Figure 2)

(Figure 3).

The band at 320 nm steadily decreases as the polymer is oxidized. Then, the absorbance in this region may be employed to quantify the fraction of oxidized polymer. Then, the relative absorbance change will be defined as:

$$\Delta A_R = \frac{A(E) - A_i}{\Delta A_T} \quad (1)$$

Where $A(E)$ is the absorbance at the potential E, A_i is the absorbance at E = -0.200 V, potential at which all the polymer is completely reduced, and ΔA_T is the total absorbance change in going from the reduced polymer to the oxidized one, measured at λ = 320 nm.

Consequently, the degree of oxidation of the polymer, θ_n, can be expressed as:

$$\theta_n = 1 - \Delta A_R \quad (2)$$

As it can be seen in Fig. 4, the relationship between ΔA_R and E depends on the solution *pH*.

(Figure 4).

4. Theoretical background

4.1 A simple model to show the coupling between the redox potential and the proton binding

The purpose of this section is to present a simple molecular model that allows showing the coupling between proton binding and the redox potential for the redox reaction represented in Scheme 1 [31–34].

(SCHEME 1).

For brevity this redox equation will be written as:

$$R \rightleftarrows Ox + \nu_e e^- + \nu_H H^+ \tag{3}$$

Where, respectively, ν_e and ν_H are the stoichiometric coefficients of electrons and protons.

The redox potential is obtained in the usual way [35] from the derivative:

$$E = \frac{RT}{\nu_e F}\left(\frac{\partial A}{\partial n_e}\right)_{T,M,N,N_{Ox}} \tag{4}$$

where A is the Helmholtz free energy of the system and n_e refers to the number of electrons participating in the reaction expressed as Eq. (3). T has the usual meaning of temperature and the quantities M, N and N_{Ox} will be defined below.

The polymer will be considered as a phase in contact on one side with a solution, the external solution, on the other, in contact with a metallic conductor capable of providing holes or electrons for the polymer to be oxidized or reduced, respectively.

The system can be depicted as a polyelectrolyte gel phase composed by intertwined polymer chains [36,37]. These chains are composed by segments; each one of them is the polymeric unit, as shown in Scheme 1. In the case of Pani, each segment is formed by four monomer units and it is considered that the polymer chains contain a total of M segments. According to the oxidation degree of the polymer,

each segment may be oxidized (in number M_{Ox}) or reduced (in number M_R), being $M = M_R + M_{Ox}$. Furthermore, as it is shown in the Scheme 1, each segment has δ redox centres that can be reversibly oxidized or reduced; n_{Ox} and n_R are the number of oxidized and reduced redox centres, respectively. The total number of them, $n = n_{Ox} + n_{R,}$ is constant. The total number of redox centres in the polymer can be expressed as $\delta M = n$, and the fraction of oxidized centres will be defined as $\theta_n = n_{Ox}/n$. Then, according to the stoichiometry of the reaction, Eq. (3) will be written as:

$$dn_{Ox} = \nu_e \, dn_e = \nu_H \, dn_H = - \, dn_R \qquad (5)$$

On the other hand, in this description of the system, it is considered that each monomer unit contains functional chemical groups capable of binding protons. In the case of Pani, these are the amine (—NH—) and the imine (—N=) groups. Depending on the proton activity of the external medium, these groups would be protonated to certain extent, giving rise to charges along the polymer chains (—NH_2^+ —) for the amine groups, and (—NH^+ =) for the imine ones. The free energy change of this process will be referred as the binding free energy, ΔA_b [36,38], and it will be considered to be at equilibrium. In turn, the charges generated along the chains by proton binding cause that the counterions present in the external electrolyte ingress into the polymer in order to maintain the electroneutrality in the space region occupied by the polymer chains. This process will be called "the charging of the polymer", and the corresponding free energy change "the electrical contribution, ΔA_{el}" [36,38]. Let be the number of H^+, bound to the M_R and M_{Ox} segments, N_R and N_{Ox}, respectively, and the total number of bound protons to be $N = N_R + N_{Ox}$. Each segment may bind χ protons. In the case of Pani, the maximum value of χ should be 4. The corresponding coverage degree of protons at the binding sites of M_R and M_{Ox} segments will be defined as $\theta_{N,R} = N_R / \chi M_R$, and $\theta_{N,Ox} = N_{Ox} / \chi M_{Ox}$, respectively.

As the polymer is progressively oxidized some M_R units become M_{Ox} units. After some number of units has been oxidized the polymer will partially become another chemical entity. For instance, in the case of Pani, after two out of four units have been oxidized, the reduced polymer (L becomes into a half oxidized polymer (E). It is assumed that during oxidation each form retains its chemical entity. That is, as

the oxidation progress the number of segments of the Leucoemeraldine form decreases and the number of segments of the Emeraldine forms increases, each one of them retaining its chemical entity.

For a polyelectrolyte gel the Helmholtz free energy can be written as the sum of four contributions [36,38]: (i) The free energy of mixing the polymer with the solvent, ΔA_m. (ii) The deformation (swelling equilibrium) free energy change, ΔA_d. (iii) The binding free energy change, ΔA_b. (iv) The electrostatic free energy, ΔA_{el}. Explicit expressions of these energies were derived in a previous publication [38].

In order to obtain the redox potential is necessary to consider the change in the Helmholtz free energy of the reaction expressed at Eq. (3). This can be written, at constant temperature and volume, as:

$$dA = \left[(\overline{\mu}_{Ox} - \overline{\mu}_R + \nu_e \overline{\mu}_e + \nu_H \overline{\mu}_H) \right] dn_{Ox} + (\mu_{N,Ox} - \mu_{N,R}) dN_{Ox} + \mu_{N,R} dN + (d\mu_{p,Ox} - d\mu_{p,R}) dM_{Ox} - d\mu_{p,R} dM_R \quad (6)$$

where, $\overline{\mu}_{Ox}, \overline{\mu}_R$, $\overline{\mu}_e$ and $\overline{\mu}_H$ are the electrochemical potential of oxidized and reduced redox centres, electrons and protons, respectively; $\mu_{N,Ox}$ and $\mu_{N,R}$ are the chemicals potentials of the proton bound sites of the oxidized and the reduced segments and $\mu_{p,Ox}$ and $\mu_{p,R}$ are the chemical potentials due to mixing and deformation of the oxidized and reduced polymer, respectively. It can be shown that, under the assumptions made, these chemical potentials are independent of M, and then of n_{Ox} [38]. Therefore, these contributions add directly to the standard part of the redox potential as constant terms.

Formally, the Nernst equation for the reaction indicated in Eq. (3) may be written as:

$$E = E^{\circ} - \frac{RT}{\nu_e F} \ln \left(\frac{a_R}{a_{Ox}} \frac{1}{(a_H)^{\nu_H}} \right) = E^{\circ} + \frac{\nu_H RT}{\nu_e F} \ln (a_H) - \frac{RT}{\nu_e F} \ln \left(\frac{a_R}{a_{Ox}} \right) \quad (7)$$

where a_j is the activity of the j species, ν_i are the corresponding stoichiometric coefficients, and E° is the standard electrode potential. The activity ratio, $\frac{a_R}{a_{Ox}}$, can be expressed in terms of the oxidized and reduced fractions and the activity coefficients, γ_i, as:

$$\frac{a_R}{a_{Ox}} = \frac{\theta_R \gamma_R}{\theta_{Ox} \gamma_{Ox}} \quad (8)$$

being $\theta_{Ox} = \theta_n$, the fraction of the oxidized redox centres, and $\theta_R = 1 - \theta_n$ the fraction of reduced redox centres. Then, E results:

$$E = E° - 2.303 \frac{\nu_H RT}{\nu_e F} pH - \frac{RT}{\nu_e F} \ln\left(\frac{\gamma_R}{\gamma_{Ox}}\right) - \frac{RT}{\nu_e F} \ln\left(\frac{1-\theta_n}{\theta_n}\right) \quad (9)$$

From Eq. (9), the formal apparent potential, E_{app}, can be defined as the part of the potential that does not depend explicitly on the concentrations of the R and Ox substances.It is important to remark that E_{app} is a magnitude experimentally accessible and does not depend on any model under consideration

$$E_{app} = E + \frac{RT}{\nu_e F} \ln\left(\frac{1-\theta_n}{\theta_n}\right) \quad (10)$$

However, taking into account the previous considerations, an expression can be obtained for this type of materials,

$$E_{app} = E° - 2.303 \frac{\nu_H RT}{\nu_e F} pH - \frac{RT}{\nu_e F} \ln\left(\frac{\gamma_R}{\gamma_{Ox}}\right) \quad (11)$$

4.2. Statistical mechanics considerations. The different chemical potentials in Eq. (6) will be obtained from the well known relationship between the Helmholtz free energy and the canonical partition function, Q; that is $A = - kT \ln Q$.

It will be assumed that the canonical partition function of the system, Q, is the product of different contributions considered being statistically independent [6]; so, it is possible to write

$$Q = Q_n Q_N Q_H Q_M \quad (12)$$

Where Q_M is the partition function of the segments, Q_N is the partition function of the bound species, Q_n is the partition function of the redox centres and Q_H is the partition function of protons in solution. Expressions for each partition function are given in Appendix A.

Then, the potential can be calculated as [6,37]:

$$E = \frac{RT}{\nu_e F}\left(\frac{\partial A}{\partial n_{Ox}}\right)_{T,M,N,N_{Ox}} = -\frac{RT}{\nu_e F}\left(\frac{\partial \ln Q}{\partial n_{Ox}}\right)_{T,M,N,N_{Ox}} \quad (13)$$

Taking into account the interaction between redox centres, within the Bragg-Williams' Approximation, the following expression for the potential can be derived (see Appendix A)

$$E = -\frac{\nu_H 2.303RT}{\nu_e F} pH - \frac{RT}{\nu_e F}\ln\left(\frac{p_{Ox}^*}{p_R^*}\left(\frac{(1-\theta_{N,R})}{(1-\theta_{N,Ox})}\right)^{\chi/\delta}\right) - \frac{\Delta\varepsilon_m}{\nu_e F}(1-2\theta_n) - \frac{RT}{\nu_e F}\ln\left(\frac{(1-\theta_n)}{\theta_n}\right) \quad (14)$$

The first term on the right hand side (rhs) of Eq. (14) shows the direct effect of the *pH* on the electrochemical reaction Eq. (3). The second term is due to the effect of proton binding (given by the term $\ln\left[(1-\theta_{N,R})/(1-\theta_{N,Ox})\right]^{\chi/\delta}$). The third term refers to the difference of interaction energy between the redox centres. Finally, the last term is the usual logarithm of the concentration ratio of the reduced over the oxidized species in the Nernst's equation Eq. (9). Replacing Eq. (14) into Eq. (10), it is possible to derive an expression for E_{app} in terms of the model

$$E_{app} = -\frac{\nu_H 2.303RT}{\nu_e F} pH - \frac{RT}{\nu_e F}\ln\left(\frac{p_{Ox}^*}{p_R^*}\left(\frac{(1-\theta_{N,R})}{(1-\theta_{N,Ox})}\right)^{\chi/\delta}\right) - \frac{\Delta\varepsilon_m}{\nu_e F}(1-2\theta_n) \quad (15)$$

4.3. **The *pH* dependence of $\Delta\varepsilon_m$**

Now, it will be analyzed the dependence of $\Delta\varepsilon_m$ on the electrolyte *pH*. For this purpose, the interaction between the redox centres will be considered coulombic in nature. And, as the intrinsic charge of segments is zero, the origin of the net charge is the protonation of the centres. This means that the second and third terms in Eq. (15) are related. Under these assumptions, the charges of oxidized and reduced segments are given by:

$$z_{Ox} = z_{H+}(\chi/\delta)\theta_{N,Ox} \quad (16)$$

And

$$z_R = z_{H+}(\chi/\delta)\theta_{N,R} \quad (17)$$

where $z_{H+}=1$ is the proton charge. Taking into account the proton binding proton isotherms and assuming that the interactions between redox centres can be considered as coulombic ones between charged spheres screened by the ionic atmosphere (see Appendix B, Eq. B.9), an expression for the $\Delta\varepsilon_m$ dependence on the solution *pH* can be derived

$$\Delta\varepsilon_m = C\left[\left(1+10^{pH-pK_{a,Ox}}\right)^{-1}-\left(1+10^{pH-pK_{a,R}}\right)^{-1}\right] \qquad (18)$$

where *C* is a constant at constant ionic strength (Eq. B.9).

5. Analysis of the Results and Discussion

According to Eq. (10) a special case of E_{app} is the value of the potential *E* at θ_n = 0.5 ($E_{\theta n=0.5}$). Fig. 5 shows these potentials, as a function of the electrolyte *pH*. As it can be seen in the figure, the dependence of E_{app} on *pH* is more complex than that predicted by the term $2.303\frac{\nu_H RT}{\nu_e F}pH$ of Eq. (11), as it would be if E^0 and γ_R/γ_{Ox} were independent of *pH*. Therefore, it should be concluded that either E^0 or γ_R/γ_{Ox}, or both, must depend on the electrolyte *pH*. This dependence comes from the coupling between the redox potential and the proton binding, mentioned at the Introduction section and on the dependence of $\Delta\varepsilon_m$ on *pH* discussed above.

(Figure 5).

(Figure 6).

In Fig. 6, E_{app} is represented as a function of θ_n for some *pH* values. This figure indicates there is an apparent potential distribution. If there was not a redox potential distribution, the plot presented in Fig. 6 would be a straight line parallel to the θ_n axis. Eq. (11) shows that the observed behaviour implies that

the ratio of the activity coefficients, γ_R/γ_{Ox}, depends on θ_n. Moreover, it is also observed that the dependence of E_{app} on θ_n is different for each *pH* value.

According to Eq. (15), a plot of E_{ap} vs. (1- $2\theta_n$) should give a straight line of slope $\Delta\varepsilon_m/\nu_e F$ and ordinate $-\frac{\nu_H 2.303RT}{\nu_e F} pH - \frac{RT}{\nu_e F}\ln\left(\frac{p^*_{Ox}}{p^*_R}\left(\frac{(1-\theta_{N,R})}{(1-\theta_{N,Ox})}\right)^{\chi/\delta}\right)$ that depends only on *pH*, as it was explained in reference to Eq. (15). Such plots are shown in Fig. 7 for different *pH* values.

(Figure 7).

Plots in Fig. 7 are approximately linear in the range $0.3 < \theta_n < 0.7$ and both the slope and the ordinate strongly depend on the *pH*. This indicates that $\Delta\varepsilon_m$ does change with *pH*. This behaviour should be expected due to the fact that the charge on the segments must change with the electrolyte *pH*. On the other hand, the ordinate is expected to depend on the electrolyte *pH* directly (first term of the rhs of Eq. (15)), and also, indirectly, through the terms $\theta_{N,R}$ and $\theta_{N,Ox}$ (see Eqs. (16), (17), (B.1), and (B.2)). The slopes and ordinates of Fig. 7 were obtained by a linear fitting procedure. The resulting values of $\Delta\varepsilon_m$, plotted against the electrolyte *pH,* are shown in Fig. 8.

In the literature there is agreement that, in the case of Pani, $\nu_e = \nu_H = 2$ [31–34], so the ordinate values determined by linear fitting can be used to calculate the term $-\frac{RT}{\nu_e F}\ln\left(\frac{p^*_{Ox}}{p^*_R}\left(\frac{(1-\theta_{N,R})}{(1-\theta_{N,Ox})}\right)^{\chi/\delta}\right)$ for each *pH* value. In order to shorten the writing, this term will be referred as E^*. Values of E^* as a function of *pH* are shown in Fig. 9. From the figure, it can be seen that the contribution of E^* to E_{app} is not negligible.

(Figure 8).

(Figure 9).

Data shown in Fig. 8 can be fitted to Eq. (18). This procedure was carried out with Levenberg–Marquardt algorithm for non-linear least squares fitting, for the parameters *C,* $pK_{a,Ox}$, and $pK_{a,R}$. The results of the fit are given in Table 1.

(TABLE 1).

Under the same assumptions considered about the nature of the interaction energy, an expression for the dependence of E^* on *pH* can be derived. In Appendix B, it is shown that:

$$E^* = A_1 + A_2\left(\left(\frac{1}{1+10^{pH-pKaOx}}\right)^2 - \left(\frac{1}{1+10^{pH-pKaR}}\right)^2\right) + A_3 \ln\left(\frac{1+10^{pH-pKaOx}}{1+10^{pH-pKaR}}\right) \quad (19)$$

where A_1, A_2, and A_3 are constants at constant temperature and ionic strength. Their expressions are given in Appendix B. Non-linear fitting of the experimental values, shown in Fig. 9, to Eq. (19) allows obtaining these constants and the *pKa* of each redox form. The resulting values are assembled in Table 2.

(TABLE 2).

According to the model, $A_3 = -\frac{\chi}{\delta}\frac{RT}{\nu_e F}$ (Appendix B). Then, from the results of the fit in Table 2, it can be estimated the relation:

$$\frac{\chi}{\delta} = \frac{-\nu_e F A_3}{RT} \approx 2 \quad (20)$$

This indicates that the number of binding sites is twice the number of redox centres, in agreement with the reaction shown in Scheme 1 (four binding sites and two redox centres per segment). The values of $pK_{a,Ox}$ and $pK_{a,R}$ listed in Table 2 are in reasonable agreement with those reported in Table 1 as well as with those reported in the literature. The value of the oxidized polymer binding constant coincides with that given in the literature [39]. The value of the reduced polymer constant is certainly smaller than the value reported by Genies *et al.* [39]. However, it deserves to be mentioned that those authors performed the titration curves on Pani synthesized chemically; experimental procedure that yields the polymer in the

shape of a fine grained powder and, therefore, it is difficult to reduce and to reach the equilibrium state. On the other hand, it has been performed an *in situ* spectrophotometrical determination employing electrosynthesized Pani films, and the $pK_{a,R}$ value obtained was about the unity for the reduced Pani (results not shown here)**.**

6. Conclusions

It was developed a simple statistical mechanic model that allows explaining the influence of proton binding on the redox potential in electrochemically active polymers. The experimental results for Pani clearly show that there is a formal redox potential distribution and it depends on pH in a complex way. The model allows explaining this dependence through the proton binding to interacting redox centers and then, quantifying the influence of binding on the redox potential. Results could be satisfactorily fitted to obtain several parameters of the system, of physicochemical interest, such as the dependence of the interaction energy between the redox centres on the electrolyte *pH* and the *pKa* values of the reduced and oxidized forms.

7. Appendix A

An expression for $\left(\partial \ln Q / \partial n_{Ox}\right)_{T,M,N,N_{Ox}}$ is needed in order to calculate the potential (Eq. (14)). Each component of the partition function, Eq. (12), will be analyzed separately.

7.1. The Partition Function of the redox centres, Q_n. Taking into account the presence of interactions between neighbour redox centres, this partition function can be written as [24,36]:

$$Q_n(n,n_{Ox},T)=\frac{n!}{(n-n_{Ox})!n_{Ox}!}\left(p_{Ox}\right)^{n_{Ox}}\left(p_R\right)^{n-n_{Ox}}\left(\exp(-\frac{\varepsilon_{OO}}{kT})\right)^{P_{OO}}\left(\exp(-\frac{\varepsilon_{RR}}{kT})\right)^{P_{RR}}\left(\exp(-\frac{\varepsilon_{OR}}{kT})\right)^{P_{OR}} \qquad (A.1)$$

where P_{ij} is the number of neighbour pairs *i-j*; p_{Ox} and p_R are the internal partition functions of the oxidized and reduced centres, respectively, when no interaction is considered [24]. Here, ε_{RR}, ε_{OO}, and ε_{OR} are the interaction energies between two *Ox* sites, two *R* sites and between one *Ox* and one *R* sites,

respectively. Within the Bragg- Williams' approximation [36] the number of neighbour pairs, P_{ij}, is calculated as [37]:

$$P_{OO} = \frac{u\left(n_{Ox}\right)^2}{2n} \tag{A.2}$$

$$P_{RR} = \frac{u(n-n_{Ox})^2}{2n} \tag{A.3}$$

$$P_{OR} = \frac{u(n-n_{Ox})n_{Ox}}{n} \tag{A.4}$$

Being u the number of closest neighbours. So, the expression for Q_n can be written as

$$Q_n(n,n_{Ox},T) = \frac{n!}{(n-n_{Ox})!n_{Ox}!}\left(p_{Ox}^*\right)^{n_{Ox}}\left(p_R^*\right)^{n-n_{Ox}}\left(\exp(\frac{\Delta\varepsilon_m}{RT})\right)^{n_{Ox}(n-n_{Ox})/n} \tag{A.5}$$

where the following definitions were employed [8]:

$$\Delta\varepsilon_m = \frac{1}{2}uN_{Av}(\varepsilon_{RR}+\varepsilon_{OO}-2\varepsilon_{OR}) \tag{A.6}$$

$$p_{Ox}^* = p_{Ox}\exp\left(-\frac{1}{2}\frac{u\varepsilon_{OO}}{kT}\right) \tag{A.7}$$

$$p_R^* = p_R\exp\left(-\frac{1}{2}\frac{u\varepsilon_{RR}}{kT}\right) \tag{A.8}$$

where N_{Av} is Avogadro's number, $\Delta\varepsilon_m$ is the energy, per mol, of formation of a pair ε_{OR}, p_{Ox}^* is the internal partition function of an Ox redox centre, p_{Ox}, with its zero energy referred to the energy ε_{OO}, and similarly for p_R^*.

Taking into account the former expressions, it can be shown that

$$\left(\frac{\partial\ln(Q_n(n,n_{Ox},T))}{\partial n_{Ox}}\right)_{T,M,N,N_{Ox}} = \ln\left(\frac{(1-\theta_n)}{\theta_n}\frac{p_{Ox}^*}{p_R^*}\right)+(1-2\theta_n)\frac{\Delta\varepsilon_m}{RT} \tag{A.9}$$

7.2. The Partition Function of the binding sites, Q_N. In order to keep the expressions as simple as possible, no interactions between occupied binding sites will be considered. Under these conditions,

$$Q_N(M, M_{Ox}, N, N_{Ox}, T) = \left[\frac{B_{Ox}!}{(B_{Ox} - N_{Ox})! N_{Ox}!} q_{Ox}^{N_{Ox}} \right] \left[\frac{(B - B_{Ox})!}{(B - B_{Ox} - (N - N_{Ox}))! (N - N_{Ox})!} q_R^{N - N_{Ox}} \right] \quad \text{(A.10)}$$

where q_{Ox} and q_R are the internal partition functions of the occupied binding sites in oxidized and reduced segments respectively, and B is the total number of binding sites ($B = \chi M$), being B_{Ox} and B_R the number of them in oxidized and reduced segments respectively. Implicitly, it was considered the partition function of the empty binding sites to be unity. Employing the Stirling's approximation, the following equation can be derived

$$\left(\frac{\partial \ln(Q_N(M, M_{Ox}, N, N_{Ox}, T))}{\partial n_{Ox}} \right)_{T, M, N, N_{Ox}} = \frac{\chi}{\delta} \ln \left(\frac{(1 - \theta_{N,R})}{(1 - \theta_{N,Ox})} \right) \quad \text{(A.11)}$$

Definitions of $\theta_{N,R}$ and $\theta_{N,Ox}$ are given in the text.

7.3. The Partition Function of the protons in solution, Q_H. By employing the stoichometric restriction given by Eq. (5), $dn_{Ox} = -\nu_H^{-1} dn_H$, it is easy to show that:

$$\left(\partial \ln Q_H / \partial n_{Ox} \right)_{T, M, N, N_{Ox}} = \nu_H \frac{\mu_H}{RT} = -2.303 \nu_H pH \quad \text{(A.12)}$$

As expected. The standard chemical potential of protons in solution is considered zero by convention [40].

7.4. The Partition Function of the segments, Q_M. Disregarding mechanical effects [24,38], the partition function of the segments does not depend on the degree of oxidation, so that, $\left(\partial \ln Q_M / \partial n_{Ox} \right)_{T, M, N, N_{Ox}} = 0$

Employing Eqs. (12) and (13), the potential can be then calculated as

$$E = -\frac{\nu_H 2.303 RT}{\nu_e F} pH - \frac{RT}{\nu_e F} \ln \left(\frac{p_{Ox}^*}{p_R^*} \left(\frac{(1 - \theta_{N,R})}{(1 - \theta_{N,Ox})} \right)^{\chi/\delta} \right) - \frac{\Delta \varepsilon_m}{\nu_e F} (1 - 2\theta_n) - \frac{RT}{\nu_e F} \ln \left(\frac{(1 - \theta_n)}{\theta_n} \right) \quad \text{(14)}$$

8. Appendix B

8.1. The binding Isotherm of the bound sites. The chemical potential of the bound species on the *Ox* sites is found by deriving the logarithm of Q_N with respect of N_{Ox}. Equating this chemical potential to the chemical potential of the protons in solution, the binding isotherm results [36]:

$$\theta_{N,Ox} = K_{N,Ox}\, a_{H+}/(1+ K_{N,Ox}\, a_{H+}) \tag{B.1}$$

Similarly, for the *R* sites, it is obtained:

$$\theta_{N,R} = K_{N,R}\, a_{H+}/(1+ K_{N,R}\, a_{H+}) \tag{B.2}$$

where $K_{N,Ox}$ *and* $K_{N,R}$ are the proton binding constants for the oxidized and reduced segments. It is important to note that $K_{a,Ox} = 1/K_{N,Ox}$ and $K_{a,R} = 1/K_{N,R}$ are the dissociation constants of the oxidized and reduced centres. Both isotherms are of the Langmuir type and this is a consequence of neglecting interactions between the bound sites.

8.2. The pH dependence of $\Delta\varepsilon_m$ and E^*. The coulombic interaction between two spherical charges 1 and 2 of radius *a*, allowing for screening effects, is [36]:

$$\varepsilon_{12}^{coul}(r>a) = \frac{z_1 z_2 e^2}{4\pi\varepsilon(1+a\kappa)}\frac{1}{r}\exp(-\kappa(r-a)) \tag{B.3}$$

where z_1 and z_2 are the magnitude of the charges, *e* is the charge of the electron, *r* is the distance between the charges, $r_D = 1/\kappa$ is the Debye length and $\kappa^2 = \left(e^2/\varepsilon kT\right)\sum_i m_i z_i^2$. $\varepsilon = \varepsilon_o\varepsilon_r$, is the dielectric constant, being $\varepsilon_o = 8.8510^{-12} C^2 N^{-1} m^{-2}$ the permittivity in vacuum and ε_R the relative dielectric constant of the medium. The sum is twice the ionic strength and m_i the molality of the *i* ionic species.

Then, assuming the redox centres are charged spheres, the coulombic interactions between them may be written as:

$$\varepsilon_{OO}^{coul}(r>a_{Ox}) = \frac{\left(z_{Ox}e\right)^2}{4\pi\varepsilon(1+a_{Ox}\kappa)}\frac{1}{r}\exp(-\kappa(r-a_{Ox})) \tag{B.4}$$

$$\varepsilon_{RR}^{coul}(r>a_R) = \frac{\left(z_R e\right)^2}{4\pi\varepsilon(1+a_R\kappa)}\frac{1}{r}\exp(-\kappa(r-a_R)) \tag{B.5}$$

$$\varepsilon_{OR}^{coul}(r > a_{OR}) = \frac{z_R z_{Ox} e^2}{4\pi\varepsilon(1+a_{OR}\kappa)}\frac{1}{r}\exp(-\kappa(r-a_{OR})) \tag{B.6}$$

where $a_{Ox} = 2r_{Ox}$, $a_R = 2r_R$, $a_{OR} = r_{Ox} + r_R$, being r_j the effective radii of the redox centre. Assuming that the mean separation distance is the same for the different centres, that the mean distance (r_m) is the same between oxidized and reduced redox centres and that the effective radii are similar, $r_{Ox} \approx r_R \approx a_m / 2$. Then:

$$\Delta\varepsilon_m^{coul} = \frac{1}{2}uN_{Av}\left(\varepsilon_{OO}^{coul} + \varepsilon_{RR}^{coul} - 2\varepsilon_{OR}^{coul}\right) = \frac{\left(z_{Ox} - z_R\right)^2 uF^2}{8\pi\varepsilon_o\varepsilon_R r_m N_{Av}(1+\kappa a_m)}\exp(-\kappa\left(r_m - a_m\right)) \tag{B.7}$$

By introducing Eqs. (B.1) and (B.2) into the expressions for the segments charges given by Eqs. (16) and (17), and employing the dissociation constants,

$$\left(z_{Ox} - z_R\right) = \frac{\chi}{\delta}\left[\left(1+10^{pH-pK_{a,Ox}}\right)^{-1} - \left(1+10^{pH-pK_{a,R}}\right)^{-1}\right] \tag{B.8}$$

being $pK_a = -\log(K_a)$. Then, assuming that $\Delta\varepsilon_m \approx \Delta\varepsilon_m^{coul}$, it results to be

$$\Delta\varepsilon_m = C\left[\left(1+10^{pH-pK_{a,Ox}}\right)^{-1} - \left(1+10^{pH-pK_{a,R}}\right)^{-1}\right] \tag{B.9}$$

where *C* is:

$$C = \frac{u(\chi F/\delta)^2}{8\pi\varepsilon_o\varepsilon_R r_m N_{Av}(1+\kappa a_m)}\exp(-\kappa\left(r_m - a_m\right)) \tag{B.10}$$

Note that *C* is constant at constant ionic strength. Note also that, in view of Eq. (B.9), for low values of *pH*, $\Delta\varepsilon_m$ tends to zero (all segments have the same charge and the difference $\left(z_{Ox} - z_R\right)$ is zero) and this parameter is maximum when the highest is the difference of protonation degree of each type of segment.

According to Eqs. (A.7) and (A.8), the quotient p_{Ox}^* / p_R^* must also depend on the state of charge and so on the *pH*. Taking into account Eqs. (B.4) to (B.6),

$$-\frac{RT}{\nu_e F}\ln\left(\frac{p_{Ox}^*}{p_R^*}\right) = -\frac{RT}{\nu_e F}\ln\left(\frac{p_{Ox}}{p_R}\right) + A_2\left(\left(1+10^{pH-pK_{a,Ox}}\right)^{-2} - \left(1+10^{pH-pK_{a,R}}\right)^{-2}\right) \tag{B.11}$$

where $A_2 = \frac{u(\chi/\delta)^2 F}{\nu_e 8\pi\varepsilon_o\varepsilon_R r_m N_{Av}(1+\kappa a_m)}\exp(-\kappa(r_m - a_m))$. Using this equation and replacing the expressions for the protonation degrees in Eqs. (B.1) and (B.2) in terms of dissociations constants, the potential E^* results:

$$E^* = -\frac{RT}{\nu_e F}\ln\left(\frac{p^*_{Ox}}{p^*_R}\left(\frac{(1-\theta_{N,R})}{(1-\theta_{N,Ox})}\right)^{\chi/\delta}\right) \qquad \text{(B.12)}$$

In terms of the *pH* and the dissociation constants, it results

$$E^* = A_1 + A_2\left(\left(\frac{1}{1+10^{pH-pKaOx}}\right)^2 - \left(\frac{1}{1+10^{pH-pKaR}}\right)^2\right) + A_3\ln\left(\frac{1+10^{pH-pKaOx}}{1+10^{pH-pKaR}}\right) \qquad (19)$$

where $A_1 = -\frac{RT}{\nu_e F}\ln\left(\frac{p_{Ox}}{p_R}\left(\frac{K_{a,R}}{K_{a,Ox}}\right)^{\chi/\delta}\right)$, and $A_3 = -\frac{\chi}{\delta}\frac{RT}{\nu_e F}$.

The three terms in Eq. (19) are as follows: the first one is a constant dependent only on the temperature. The second one is related to the dependence of the interaction energies between the redox centres on the *pH* whereas the third one is related to the dependence of the binding process on the *pH*.

9. Acknowledgments

This work was financially supported by the Consejo Nacional de Investigaciones Científicas y Técnicas (PIP 0813), the Agencia Nacional de Promoción Científica Tecnológica (PICT-0407) and the Universidad Nacional de La Plata (UNLP) (Proyecto 11/X590). MIF and DP are members of the CIC of the CONICET. WAM thanks a fellowship of CONICET.

10. References

[1] G. Zubay, Biochemistry, 4th ed., Wm. C. Brown, New York, 1998.

[2] R.W. Murray, ed., Molecular Design of Electrode Surfaces, Wiley, New York, 1992.

[3] M.E.G. Lyons, Electroactive Polymer Electrochemistry, Plenum, New York, 1996.

[4] P. Chandrasekar, Conducting Polymers, Fundamentals and Applications, Kluwer Academic Publishers, Norwell, MA, 1999.

[5] Y. Bar-Cohen, ed., Electroactive Polymer(EAP) Actuators as Artificial Muscles: Reality, Potential, and Challenges, 2nd ed., SPIE, Washington, 2004.

[6] W.A. Marmisollé, M. Inés Florit, D. Posadas, Phys. Chem. Chem. Phys. 12 (2010) 7536–44.

[7] C. Tanford, J.G. Buzzell, D.G. Rands, S.A. Swanson, J. Am. Chem. Soc. 77 (1955) 6421–6428.

[8] C. Tanford, J. Phys. Chem. 59 (1955) 788–793.

[9] G. Ybarra, C. Moina, F. V Molina, M.I. Florit, D. Posadas, Electrochimica Acta 50 (2005) 1505–1513.

[10] J. Mazur, A. Silberberg, A. Katchalsky, J. Polym. Sci. 35 (1959) 43–70.

[11] A. Katchalsky, J. Mazur, P. Spitnik, J. Polym. Sci. 23 (1957) 513–532.

[12] J.G. Voet, J. Coe, J. Epstein, V. Matossian, T. Shipley, Biochemistry 20 (1981) 7182–7185.

[13] L. Lizarraga, E.M. Andrade, F.V. Molina, Electrochim. Acta 53 (2007) 538–548.

[14] L. Lizarraga, E.M. Andrade, F. V. Molina, J. Electroanal. Chem. 561 (2004) 127–135.

[15] J. Petrović, R. a Clark, H. Yue, D.H. Waldeck, E.F. Bowden, Langmuir 21 (2005) 6308–16.

[16] M. Tagliazucchi, F.J. Williams, E.J. Calvo, J. Phys. Chem. B 111 (2007) 8105–8113.

[17] T. Pascher, B.G. Karlsson, M. Nordling, B.G. Malmstrom, T. Vanngard, Eur. J. Biochem. 212 (1993) 289–296.

[18] M. Tagliazucchi, E.J. Calvo, I. Szleifer, Langmuir 24 (2008) 2869–2877.

[19] R. Margalit, A. Schejter, Eur. J. Biochem. 499 (1973) 492–499.

[20] G. Battistuzzi, M. Borsari, D. Dallari, I. Lancellotti, M. Sola, Eur. J. Biochem. 241 (1996) 208–214.

[21] W. Qian, Y.-H. Wang, W.-H. Wang, P. Yao, J.-H. Zhuang, Y. Xie, Z.-X. Huang, J. Electroanal. Chem. 535 (2002) 85–96.

[22] F.A. Leitch, G.R. Moore, G.W. Pettigrew, Biochemistry 23 (1984) 1831–1838.

[23] S.W. Feldberg, J. Am. Chem. Soc. 106 (1984) 4671–4674.

[24] W.A. Marmisollé, M.I. Florit, D. Posadas, J. Electroanal. Chem. 655 (2011) 17–22.

[25] W.A. Marmisollé, M.I. Florit, D. Posadas, J. Electroanal. Chem. 660 (2011) 26–30.

[26] W.A. Marmisollé, D. Posadas, M.I. Florit, J. Phys. Chem. B 112 (2008) 10800–5.

[27] P.M. McManus, S.C. Yang, R.J. Cushman, J. Chem. Soc. Chem. Comm. (1985) 1556–1557.

[28] D.E. Stilwell, S. Park, J. Electroanal. Chem. 136 (1989) 427–433.

[29] D. Chinn, J. DuBow, J. Li, J. Janata, M. Josowicz, Chem. Mater. 7 (1995) 1510–1518.

[30] A.A. Nekrasov, V.F. Ivanov, A. V. Vannikov, J. Electroanal. Chem. 482 (2000) 11–17.

[31] W.S. Huang, A.G. MacDiarmid, Polymer 34 (1993) 1833–1845.

[32] E.M. Genies, M. Lapkowski, C. Tsintavis, New J. Chem. 12 (1988) 181–196.

[33] G. Inzelt, G. Horányi, Electrochim. Acta 35 (1990) 27–34.

[34] M. Kalaji, L. Nyholm, L.M. Peter, J. Electroanal. Chem. 313 (1991) 271–289.

[35] P.D. Atkins, Physical Chemistry, 6th ed., Oxford University Press, Oxford, 1998.

[36] T.L. Hill, An Introduction to Statistical Thermodynamics, Addisson-Wesley Reading, MA, 1960.

[37] D. Posadas, M. Fonticelli, M.J. Rodriguez Presa, M.I. Florit, J. Phys. Chem. B 105 (2001) 2291–2296.

[38] D. Posadas, M.I. Florit, J. Phys. Chem. B 108 (2004) 15470–15476.

[39] E.M. Genies, E. Vieil, Synth. Met. 20 (1987) 97–108.

[40] K.G. Denbigh, The Principles of Chemical Equilibrium, 4th ed., Cambridge University Press, Cambridge, 1981.

Captions of Figures and Schemes

SCHEME 1: Redox commutation for the first redox couple of Pani (only the base forms are shown).

Figure 1. Schematic representation of the ITO electrode and the cell arrangement.

Figure 2. Voltammetric current potential relationships for a Pani film at different sweep rates, ν / Vs^{-1}: 0.002, 0.005, 0.01, 0.025, 0.05, and 0.1. Electrolyte: 3.7M H_2SO_4. Q_T (0.45) = 32.0 mC cm^{-2}.

Figure 3. Pani spectra at different potentials comprised between -0.2 and 0.45 V in 3.7 M H_2SO_4 (pH = -0.60). The arrows indicate the direction of increasing potentials. Q_T (0.45) = 32 mC cm^{-2}.

Figure 4. Relative absorbance changes of the 320 nm band as a function of the applied potential for different *pHs*. Q_T (0.45) = 32 mC cm^{-2}. (●) - 0.60, (○) 0.87, (▼) 1.31, (△) 2.31.

Figure 5. Dependence of $E(\theta_n = 0.5)$ on the electrolyte pH values.

Figure 6. Dependence of E_{ap} on θ_n for data of Fig. 4.

Figure 7. Plot of E_{ap} against $(1- 2\theta_n)$ at different pH values. (●) - 0.60, (○) – 0.02, (▼) 0.20, (△) 0.71, (■) 1.01, (□) 1.48, (◆) 2.31, (◇) 3.32.

Figure 8. Dependence of $\Delta\varepsilon_m$ on the pH. The line is the result of the fit to Eq. (18).

Figure 9. E^*, calculated from the ordinates of Fig. 7, as a function of pH. The line is the result of the fit to Eq. (19).

Figures and Schemes:

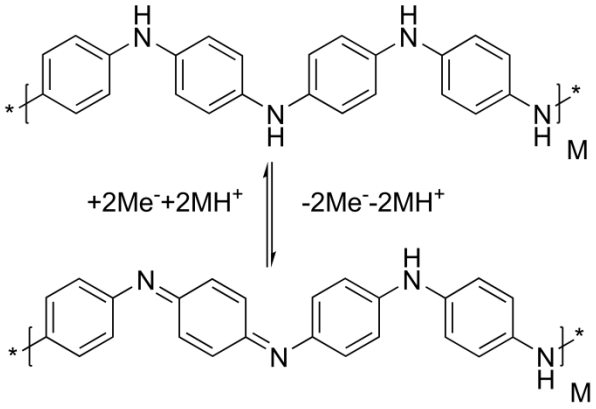

SCHEME 1

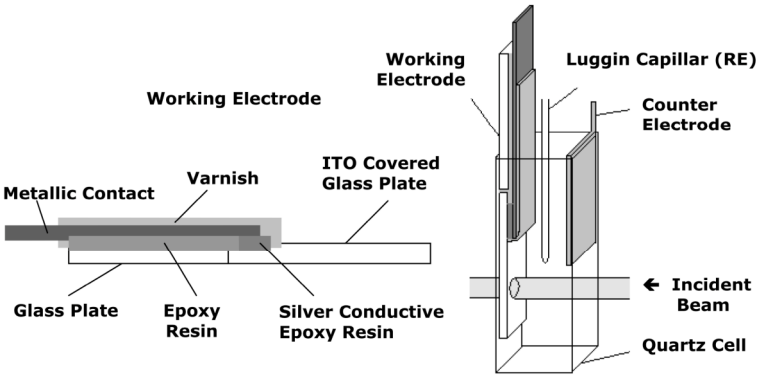

Figure 1

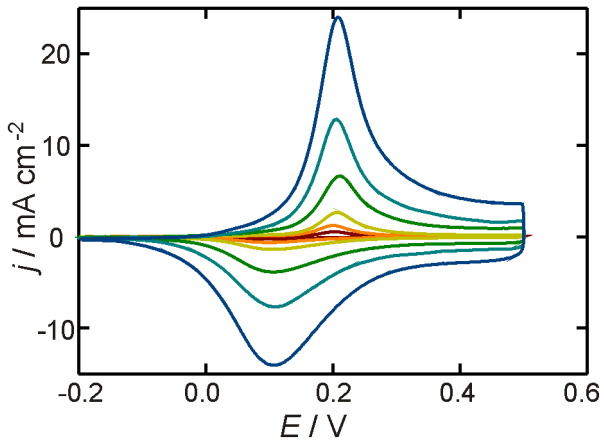

Figure 2

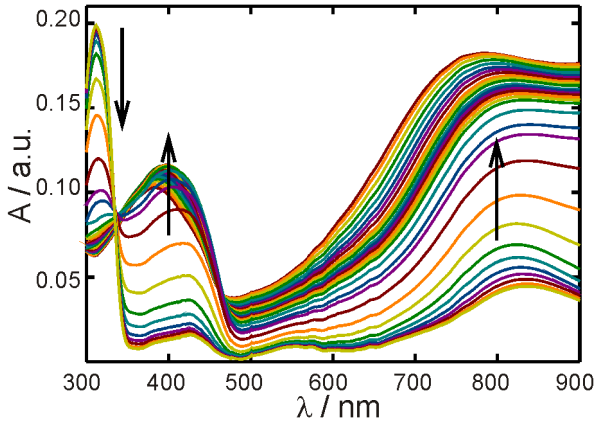

Figure 3

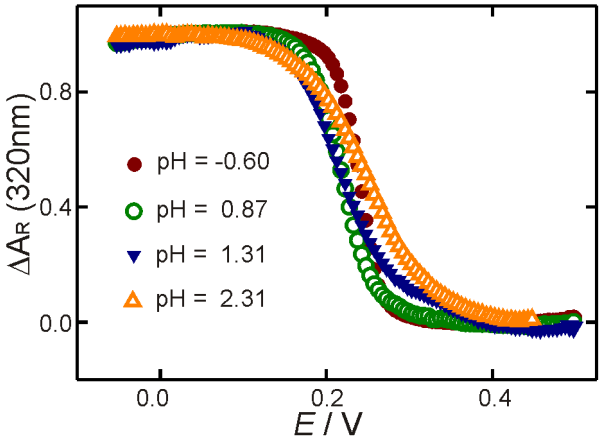

Figure 4

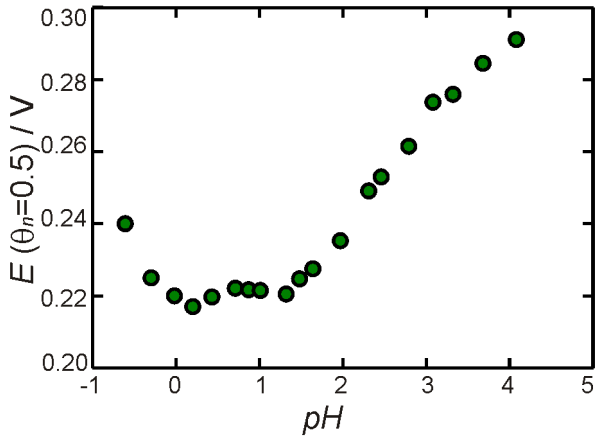

Figure 5

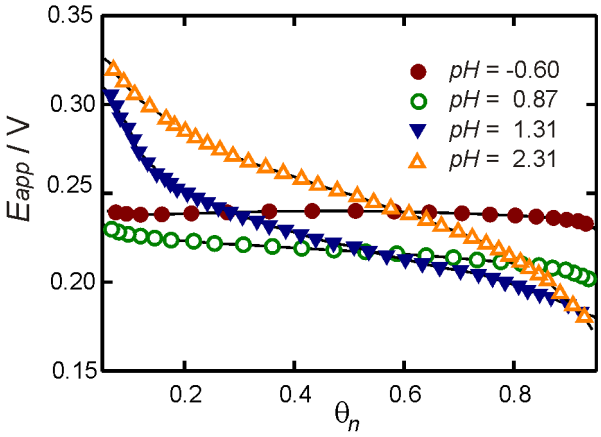

Figure 6

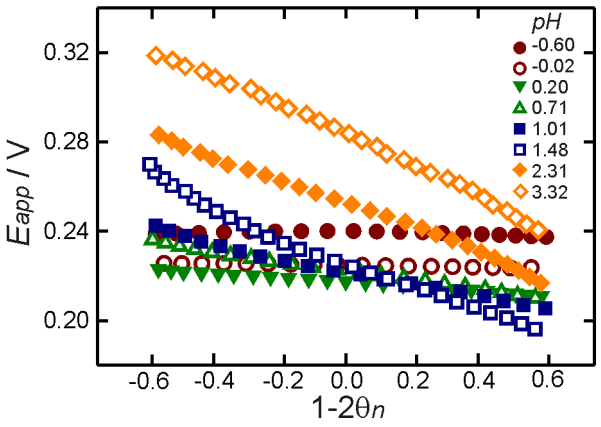

Figure 7

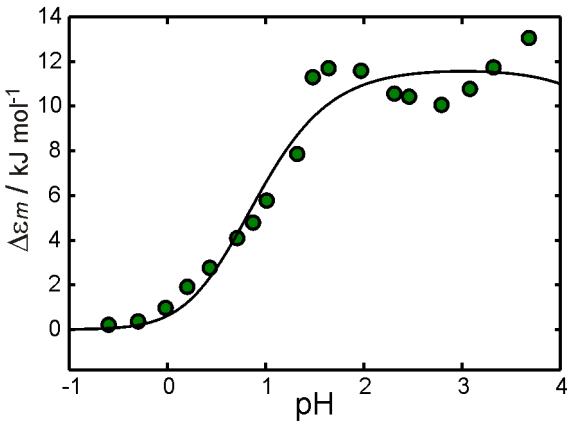

Figure 8

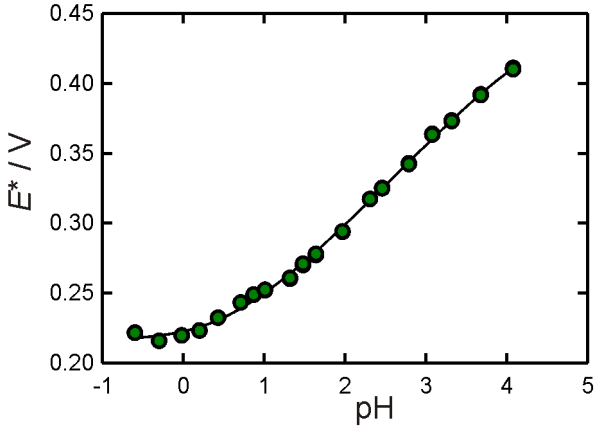

Figure 9

Tables:

Table 1: Results of the fit of data in Figure 8 to Eq. (18)

B / $kJmol^{-1}$	$pK_{a,Ox}$	$pK_{a,R}$	r^2
11.8±0.6	5.5±1.5	0.52±0.07	0.987

[a] r^2 is the correlation coefficient of the fit.

Table 2: Results of the fitting of the data of E^* and pH according to Eq. (19) [a]

A_1 / V	A_2 / V	A_3 / V	$pK_{a,Ox}$	$pK_{a,R}$	r^2
0.2162±0.002	0.015±0.01	- 0.0257±0.0006	4.8±0.3	0.9±0.2	0.9998

[a] r^2 is the correlation coefficient of the fit.